Desalination 545 (2023) 116159

Contents lists available at ScienceDirect

Desalination

journal homepage: www.elsevier.com/locate/desal

Polyelectrolyte multilayers coating of aliphatic polyamide anion-exchange membranes to increase monovalent/divalent anions selectivity in electrodialysis

Muhammad Ahmad [a,*], Mahmood Ahmed [a,*], Shabbir Hussain [b], Abid Ali [c], Manzar Zahra [d], Muhammad Imran Din [e], Zeeshan Mustafa [f]

[a] Department of Chemistry, Division of Science and Technology, University of Education, Lahore 54770, Pakistan
[b] Institute of Chemistry, Khawaja Fareed University of Engineering and Information Technology, Rahim Yar Khan, Pakistan
[c] Department of Chemistry, The University of Lahore, Lahore 54000, Pakistan
[d] Department of Chemistry, Lahore Garrison University, Lahore, Pakistan
[e] Centre for Physical Chemistry, School of Chemistry, University of the Punjab, Lahore 54590, Pakistan
[f] Department of Physics, Lahore Garrison University, Lahore, Pakistan

HIGHLIGHTS

- Deposition of PAH/PSS-films on anion-exchange membranes increases the Cl^-/SO_4^{2-} ED selectivity up to 180.
- Increase in Cl^-/SO_4^{2-} selectivity is highly dependent on the feed concentrations and the applied currents.
- As high as 90 % current efficiencies are achieved in ED separations in the Ohmic region.
- Polyelectrolyte multilayers facing either the source or the receiving phase show different selectivities.
- Coatings terminated with polycations show much lower anion selectivities than those terminated with polyanions.

GRAPHICAL ABSTRACT

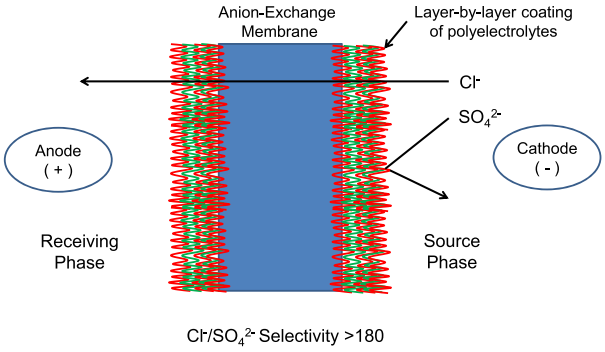

ARTICLE INFO

Keywords:
Anion-exchange membranes
Polyelectrolytes
Selectivity
Electrodialysis

ABSTRACT

Layer-by-layer (LBL) modification of aliphatic polyamide anion-exchange membranes (AEMs) with poly(4-styrenesulfonate) (PSS) and protonated poly(allylamine) (PAH) coatings increases monovalent/divalent anion transport selectivities. Remarkably, in electrodialysis (ED) Cl^-/SO_4^{2-} selectivities increase from 1.3 to ~180. In addition, current efficiencies reach ~90 %. Selectivity, however, decreased to ~50 when the Cl^-/SO_4^{2-} source-phase ion concentrations increased from 10 to 100 mM and from ~180 to ~10 when the current density went up from 0.63 to 2.23 mA·cm^{-2}. The current efficiency also went down to ~50 % at 2.23 mA cm^{-2} which indicates the introduction of some parasitic phenomenon at higher current densities. Moreover, for a coated membrane, the polyelectrolyte multilayer (PEM) coating facing the source phase is comparatively more selective in ED whereas the PEM facing the receiving phase is relatively more selective in diffusion dialysis (DD). Also, the $(PSS/PAH)_{11}$–films (11 bilayers of PSS and PAH polyelectrolytes) which are terminated in polycations show much

* Corresponding authors.
E-mail addresses: dr.muhammad.ahmad@ue.edu.pk (M. Ahmad), mahmood.ahmed@ue.edu.pk (M. Ahmed).

https://doi.org/10.1016/j.desal.2022.116159
Received 20 July 2022; Received in revised form 19 September 2022; Accepted 2 October 2022

lower Cl^-/SO_4^{2-} selectivity and current efficiency as compared to the $(PSS/PAH)_{10}$PSS-films (10 bilayers of PSS and PAH polyelectrolytes capped with a layer of PSS polyelectrolyte) which are terminated in polyanions. These relatively inexpensive but highly selective and current efficient AEMs can be used in ED for the purification of salts containing divalent and/or multivalent anions.

1. Introduction

Highly selective ion separation methods are gaining much importance in this modern era of technology because of their enormous potential to supply materials for devices such as batteries and high performance magnets [1,2]. Traditional techniques (e.g. precipitation and solvent extraction) can be useful to perform ion-separations, but the requirements of long evaporation times and/or toxic chemicals can preclude the use of these techniques on a wider scale [3]. Ion separations through membranes can be performed continuously often without involving any addition of external reagents [4]. Particularly, monovalent ion permselective (MIP) ion-exchange membranes (IEMs) reject divalent and multivalent ions while permitting passage of only monovalent ions [5–10]. Highly monovalent to divalent (or monovalent to multivalent) selective IEMs can be employed in electrodialysis (ED) to remove sulfate ions and hence to enhance the quality of edible salt [11,12]. In ED, an applied electrical current drives anions and cations through IEMs from diluate to concentrate compartments. Therefore, MIP membranes can play a prime role in the separation of ions of different valence in ED. Some other important areas where MIP membranes can extend the applications of ED include separation and purification of mixtures of different salts [13], avoidance of crossover of vanadium in redox flow batteries [14], electrochemical addition of acid to food products to prolong their life spans [15], divalent ions (Ca^{2+} and Mg^{2+}) removal to treat the water hardness [16], and acid recoveries from the industrial wastes having metallic salts [17].

Highly permselective IEMs can further increase the importance of ED by yielding current-efficient separations of ions. However, a typical cation-exchange membrane (CEM) demonstrates a lower selectivity among cations of different valence and a typical anion-exchange membrane (AEM) shows a lower selectivity among anions of different valence. Many studies have reported increased selectivities through IEMs in dialysis experiments by depositing highly selective coatings [5,18–21]. The sign of the fixed charge of a coating matches to that of the IEM counterions [22]. Due to electrostatic forces of repulsions, counterions for the IEM are excluded [23]. The electrostatic exclusions are particularly high for divalent and multivalent ions and thus coatings may selectively exclude divalent and multivalent ions because of their large hydrated radii and hydration energies [24–26]. A large number of studies indicate that layer-by-layer (LBL) deposited polyelectrolyte films can serve as highly selective thin films for separation membranes [27–29]. The stability of the deposited film for the separation of ions comes from hydrophobic interactions and an increased entropy due to release of counterions [30,31].

In some studies, the monovalent ion permselectivity of membranes has been increased by increasing the crosslinking density of a membrane's matrix. Thus, ions of larger hydrated radii feel more hindrance during their movement across an IEM. Ge and coworkers added a dense top layer onto the surface of a nanofiltration membrane to increase the crosslinking density of membrane's matrix and reported a selectivity of 7 in a Na^+ to Mg^{2+} separation during ED [32]. However, scaling due to formation of precipitates of multivalent ions onto the surfaces of such modified membranes can greatly reduce the fluxes of ions of interest [33,34]. The LBL deposition of PEMs provides a net charge to the coating and hence the scaling process may be decreased considerably due to electrostatic forces of repulsions present between a membrane's surface and the precipitates of multivalent ions [30,35].

LBL deposition of polyelectrolyte multilayers was employed by a large number of research studies to obtain a selective transport of ions through IEMs by varying the thickness, swelling and charge density of the membrane coating. Abdu et al. deposited thin films on a Neosepta CMX IEM by employing LBL deposition of polyethylenimine(PEI)/PSS polyelectrolytes to increase the Na^+ to Ca^{2+} ED selectivity from 0.64 to 1.5 while minimizing the transport resistance of ions through membranes [36]. In another study, a layer of PEI film was electrochemically deposited on Nafion cation-exchange membranes (CEMs) to achieve a Na^+/Cr^{3+} selectivity >10 [37]. White and coworkers also employed the same LBL method to deposit five and half bilayers of PAH/PSS polyelectrolytes on Nafion CEMs and remarkably increased the monovalent to divalent and monovalent to multivalent cation selectivities >1000 [19,20]. Zhu et al. used cost effective Fujifilm CEMs and deposited 5.5 bilayers of PAH/PSS polyelectrolytes by LBL method and achieved the same remarkable selectivities of >1000 [9]. Yang and coworkers modified Nafion CEMs with the deposition of 5.5 bilayers of PAH/PSS polyelectrolytes to improve selectivity among monovalent cations in dialysis experiments [10].

A number of recent studies also employed the LBL deposition method to modify anion-exchange membranes (AEMs) to increase the monovalent to divalent (or monovalent to multivalent) anions transport selectivities. Pan et al. deposited a layer of polyethyleneimine electrochemically on the surface of an AEM and then immobilized it covalently to achieve monovalent to divalent anions selectivity upto 4.27 [38]. Zhang et al. used interfacial polymerization to graft a thin electronegative layer on an AEM's surface and thus increased Cl^-/SO_4^{2-} selectivity to 10.3 from 1.8 [39]. Liu and coworkers crosslinked the deposited polyelectrolyte multilayers to improve the stability of deposited film and reported a selectivity to 4.36 through these films [40]. Zhao et al. used electric pulse deposition method to modify AEM by depositing layers of N-O-sulfonic acid benzyl chitosan and hydroxypropyl trimethyl ammonium chloride chitosan and achieved Cl^-/SO_4^{2-} selectivity up to 47 during first 20 min of ED [41]. In another study [7], Fujifilm type-1 AEMs were coated with 5.5 bilayers of PAH/PSS polyelectrolytes and Cl^-/SO_4^{2-} selectivity as high as 140 was reported for the source phase containing 0.1 M of each NaCl and Na_2SO_4. The authors reported that an increase in monovalent/divalent anions selectivity was highly dependent on the source phase salt concentrations. The modified AEMs demonstrated an increase in Cl^-/SO_4^{2-} selectivity from 1.7 to 5.3 when the source phase contained 0.01 M concentration with respect to each NaCl and Na_2SO_4.

A detailed review of the literature indicates that ion transport selectivities through ion-exchange membranes coated with polyelectrolyte multilayers increases appreciably. But the problem is that the current efficiency in the electrodialysis decreases due to an increased hindrance to mass transport through polyelectrolyte multilayer coated membranes. Therefore, a comprehensive study is required to better understand the effect of various factors on the transport of ions across AEMs in electrodialysis experiments. A number of factors such as current density, source phase concentration and the side of coating can play a prime role on the fluxes of anions, their selectivities and current efficiencies in ED. An estimation of the value of limiting current is also important to make ED separations of anions as current efficient. Moreover, it is imperative to explore relatively inexpensive anion-exchange membranes to decrease the cost of ED separations. In addition, we need to further increase the monovalent to divalent anion selectivities to increase the usefulness of AEMs in ED.

In this study, we have employed relatively inexpensive Fujifilm type-1 anion-exchange membranes and performed their modification by depositing 10.5 bilayers of PAH/PSS polyelectrolytes to completely

cover and modify the inhomogeneous surfaces of the membranes. Such a modification of AEMs remarkably increases the monovalent/divalent anions selectivity in ED. The ED and DD selectivities are comparatively higher than those reported in the literature. We measured an estimated value of the limiting current using *I-V* curves method and then we performed ED separations at different current densities to see the effect of current density on the fluxes of ions, selectivities and current efficiency in the Ohmic, plateau and overlimiting zones.

Next, we performed a range of experiments to better understand the transport phenomenon of cations and anions across an AEM in the electrodialysis experiments. We also tried to decrease the hindrance to mass transport by coating the membranes on only one side and thus measured the difference in selectivity due to the PEM coating either facing the source phase or the receiving phase. Finally, we performed ED in a 2-compartment cell and compared its performance with that of a 3-compartment cell and figured out the reasons behind the differences in the performances of both cells.

2. Experimental

2.1. Materials

Sodium sulfate, poly(sodium 4-styrenefulfonate, Mw = 70,000 Da), and poly(allylamine hydrochloride, Mw = 17,500 Da) were acquired from Sigma-Aldrich. Jade Scientific provided the sodium chloride and potassium chloride. Potassium sulphate was acquired from VWR, whereas sodium bicarbonate and sodium carbonate were procured from Columbus Chemicals. All the chemicals were used as received, whereas all solutions were prepared using DI H_2O (Milli-Q reference Ultra-pure Water Purification System, 18 M cm). The pH levels of the both PSS and PAH polyelectrolyte solutions were adjusted using 0.1 M solutions of HCl and NaOH. Fujifilm type-1 cation-exchange membranes and Fujifilm type-1 anion-exchange membranes were purchased from Fujifilm. Alumina membranes (pore size = 20 nm, diameter 25 mm) were purchased from Whatman.

2.2. Characterization of CEMs and AEMs

A Magellan 400 FESEM (field-emission scanning electron microscope) was used to take images of bare and coated membranes. The AEM samples were dried for 24 h at 30 °C in a vacuum oven and were sputter coated with 2 nm thick iridium layers before taking images.

The ion exchange capacities (IECs) of CEMs and AEMs were measured by immersing them in 0.1 M KCl solution for 3 days and the solutions changed to fresh solutions after every 24 h to equilibrate the membranes with the solution. After equilibration, the excess solution was removed by rinsing the membranes for ~6 s with DI H_2O from a wash bottle. Next, the AEMs were soaked in 50 mL solution containing 0.01 M $NaHCO_3$ and 0.1 M Na_2CO_3 for 2 days to remove the Cl^- ions from AEMs into the solution and CEMs were soaked in 50 mL solution containing 0.1 M NaCl for 2 days to remove K^+ ions from the CEMs into the solution. The concentration of Cl^- in AEMs was measured with ion chromatography and the concentration of K^+ in CEMs was measured with ion coupled plasma optical emission spectroscopy. The ion exchange capacities of the membranes were measured by calculating the total mmol of ions displaced from the membranes and then dividing them with the dry weights of membranes.

Resting drop method [42] was used to determine the water contact angles of the swollen surfaces of AEMs and CEMs. The distilled H_2O was used as a test liquid. After the test drop touched the surface of the AEMs and CEMs, the water contact angle was measured in 20 s.

2.3. Polyelectrolyte multilayered film deposition and thickness measurement

A mechanical die was used to punch Fujifilm cation- and anion-exchange membranes into 25-mm disks. The punched membranes were kept in a 0.01 M NaCl solution overnight for pretreatment. Membranes were thoroughly rinsed with DI H_2O after pretreatment with a squirt bottle. For modification, AEMs were soaked in PSS and PAH solutions alternatively for approximately 10 min. The solutions of both PSS and PAH polyelectrolytes were prepared in 0.5 M NaCl while the concentrations of repeat units in both polyelectrolyte solutions were 25 mM. The pH of the polyelectrolyte solutions was set to ~2.3 with 0.1 M NaOH and 0.1 M HCl solutions. The AEMs were thoroughly rinsed with DI H_2O for 30 s to remove weakly attached polyelectrolytes in between any two adsorptions of polyelectrolyte layers. A Teflon O-ring holder was used to coat only one side of the AEMs where just one side of the AEM was exposed to the polyelectrolyte and rinsing solutions.

Au-coated Si wafers were employed to measure the $(PAH/PSS)_{10}PAH$ film thickness using ellipsometry. Initially, the wafers were cleaned for 15 min in a UV/O_3 chamber and were then immersed in 0.005 M ethanolic solution of 3-Mercaptopropionic acid (MPA) overnight. After depositing a layer of MPA, wafers were rinsed with DI H_2O and C_2H_5OH. Next the wafers were dried with N_2 gas and these modified wafers served as a substrate for the deposition of $(PAH/PSS)_{10}PAH$ films. The coating of the wafers started with the deposition of PAH layer, where wafers were immersed in 25 mM PAH solution prepared in a 0.5 M NaCl as a supporting electrolyte (pH 2.3) for 10 min. After depositing PAH layer, wafers were thoroughly rinsed with DI H_2O from a squirt bottle for 30 s. Next the wafers were immersed in PSS solution of same strength, pH and supporting electrolyte. The deposition of polyelectrolytes was repeated to deposit the $(PAH/PSS)_{10}PAH$-film where the wafers were thoroughly rinsed with DI H_2O between any two consecutive adsorptions. A spectroscopic ellipsometer (alpha-SE, J.A. Woollam) was used to measure the dry thickness of the deposited film at an incident angle of 70°. Before performing in situ ellipsometry, the modified Au-coated wafers were soaked in the 0.01 M solution with respect to each NaCl and Na_2SO_4 for 90 min. in a 500 μL liquid cell (J.A. Woollam). Cauche model was used to fit film refractive indices in these experiments. The model specified DI H_2O as the ambient medium (25 °C) for films in solution. In a prior experiment, the gold substrate n and k values were determined in air. Three replicate films on three different wafers were used to perform ellipsometric measurements on two or three spots for each wafer.

2.4. Measurement of current-voltage (I-V) curves

I-V curves were measured in a home-made 2-compartment cell similar to that for ED. A potential was applied across the platinum electrodes inserted into the source and receiving phases to generate a constant current across the membrane. The voltage drop across the AEM was measured with the help of a multimeter attached to Ag/AgCl reference electrodes which were sealed into Luggin capillaries. The capillaries were kept close to the membrane's surface (within 4 mm) to minimize the voltage drop through the solution. The values of current densities ranged from 0 to 3 mA/cm^2 and the potential drop across the membrane was measured from the potential difference between Ag/AgCl reference electrodes at an applied current density value. Both the receiving and source phases were 0.01 M with respect to NaCl and 0.1 M with respect to Na_2SO_4. The phases were stirred vigorously throughout the measurements to keep the concentration polarization minimum near the membrane's surface. In a similar way, the resistance of bare AEM was measured by obtaining a plot between an applied current density and the potential drop across the membrane. The reciprocal of the resistance yielded conductance of the membrane.

2.5. Electrodialysis

A homemade electrochemical cell having three separate 100 mL glass compartments was used to separate Cl^- and SO_4^{2-} ions. The compartments were clamped together with O-rings (Fig. 1) and the exposed area of membranes was 3.1 cm^2 in these cells. An electric potential was

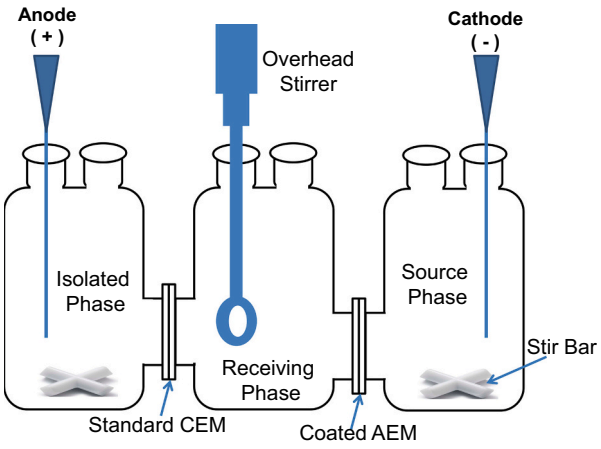

Fig. 1. Homemade ED setup consisted of three 100 mL glass compartments filled with respective phases. To avoid leaking, compartments were joined by 2.5 cm number 15 flat joints having embedded tracks for O-rings.

applied to two platinum wires inserted into the solutions of outer two compartments, such that anode was dipped in an isolated compartment (containing 0.01 M Na_2CO_3 initially) whereas cathode was dipped in the source phase. The central compartment initially contained 0.01 M Na_2CO_3 as a receiving phase. A bare pretreated CEM was inserted between the receiving and the isolated anodic compartments and the coated AEM was inserted between the receiving and source phases. Under an applied potential, anions move from the source to receiving (central) compartment but a CEM blocks their migration from receiving to the isolated phase. Cations migrate through CEM from isolated anode to the receiving phase. A potentiostat (CH instrument model 604) was used to produce a constant current density of 0.63 mA cm^{-2} across the membranes by applying the potential across a resistor (499 Ω). The resistor was attached to the reference and working electrodes. The potentiostat's reference terminal was attached to the Pt anode inserted in the isolated phase compartment whereas counter terminal of potentiostat was attached to Pt cathode inserted in the source phase [20]. In some studies, applied voltage was increased or decreased to generate lower or higher current densities by employing the same 499 Ω resistor. A vigorous stirring of all the phases was performed during dialysis experiments to keep the concentration polarization minimum near the membrane's surface. The purpose of using an isolated compartment was to avoid the formation of Cl_2 gas in ED due to oxidation of Cl^- ions on anode which can potentially damage the polyelectrolyte film deposited on the AEM [43]. 1 mL sample aliquots were withdrawn from the receiving compartment periodically during 2 h of ED. Equal volumes in all the compartments were maintained by withdrawing corresponding aliquots from the source and isolated phases as well. Ion chromatography (Thermo Dionex ICS-5000 Ion Chromatograph) was employed to determine the concentration of target anions whereas source phase concentrations were also analyzed occasionally. The calibration curves were obtained by using a number of dilutions with DI H_2O of a seven-anion standard solution (Thermo Fisher, USA). In some experiments, ICP-OES (inductively coupled plasma-optical emission spectroscopy, Perkin Elmer Optima 8000 Prep 3) with calibration curves was used to determine the concentrations of cations. For diffusion dialysis, the same three compartment cell was employed without any applied current.

The amounts of Cl^- and SO_4^{2-} ions permeated through the bare and coated AEMs were plotted against time. The fluxes of anions of interest were estimated by dividing the slopes of these plots by a membrane's exposed area. To allow steady state to occur, slopes were measured only from the data points obtained after 30 min in a 120 min dialysis experiment. When the source phase contained equal concentrations of Cl^- and SO_4^{2-} ions, the Cl^-/SO_4^{2-} selectivities were determined by dividing the flux of Cl^- with that of SO_4^{2-}.

The minimum calculated selectivities are shown as $>$ values with the limit as the smallest selectivity from three different AEMs because the calculated selectivities show large deviations due to variations in the low multivalent ions fluxes.

The transference number, t_i, was determined by employing Eq. 1 [20,43], where J_i is the molar flux of ion i, z_i is the ion charge, F is the Faraday constant, and I is the current density.

$$t_i = \frac{J_i x z_i x F}{I} \quad (1)$$

Eq. (1) employs the total ion flux, which may occur either due to diffusion or the applied current. Therefore, this method overestimates t_i values when diffusive transport is significant (see the results and discussion section for more details).

3. Results and discussion

Fujifilm ion-exchange membranes are made up of an aliphatic polyamide matrix which is impregnated in a fibrous support. Firstly, this section shows the surface morphology study of bare and coated Fujifilm AEMs and then explores the remarkable improvement in transport selectivity of anions that results from LBL deposition of PEMs on these substrates. In addition, we estimate current efficiencies and examine if selectivities and current efficiencies depend on whether films terminate in a polycation or a polyanion. Later subsections investigate limiting currents and the effect current density and source phase concentration on selectivities.

3.1. Characterization of Fujifilm anion-exchange membranes

Deposition of defect-free polyelectrolyte films requires IEMs having smaller pore sizes (diameters <20 nm) [44]. Fig. 2 shows some SEM images of Fujifilm type-1 AEMs. Although these membranes do not demonstrate especially coarse surfaces, they carry some channels of widths of 10's of micrometers (please see Fig. 2 C). A LBL deposition of PEMs likely covers both the upper surfaces and the channels. Indeed, one of the impressive features of LBL deposited films is conformal coverage of 3-dimensional surfaces [45]. Images of modified membranes show small nodules that are probably polyelectrolyte complexes that form during the LBL deposition of polyelectrolyte layers. The presence of these nodules in both channels and on the surface may indicate coverage of the entire membrane.

The SEM images of the coated membranes were taken when they were dry but their modification was performed in the wet form. The IEMs swell due to excess intake of water when they are wet but shrink due to the evaporation of water when they get dry. The undulating patterns as shown in Fig. 2D are likely formed because of the evaporation of water and thus a decrease in the volume of the membrane. Image 2F was taken to see if the PEMs cover the inner sides of the channels. The image shows the deposition and stacking of the polyelectrolyte multilayers both on the surface as well as inside the channels. In this figure, the nodules of the polyelectrolyte complexes can be seen both on the surface as well as inside the channels of the membranes.

The IECs of the AEMs and CEMs were estimated by calculating the total mmol of ions displaced from the membranes and then dividing them with the dry weights of membranes. The IECs were found to be 1.63 ± 0.6 mmol/g and 1.48 ± 0.5 mmol/g for the AEMs and CEMs respectively.

Resting drop method was used to measure the contact angle of CEMs and AEMs and it was found to be 36.5 ± 2.4° and 29.8 ± 1.9° for CEMs and AEMs respectively.

3.2. Measurement of $(PAH/PSS)_{10}PAH$ film thickness and ion permeability coefficients

Ellipsometry was used to measure the $(PAH/PSS)_{10}PAH$-film

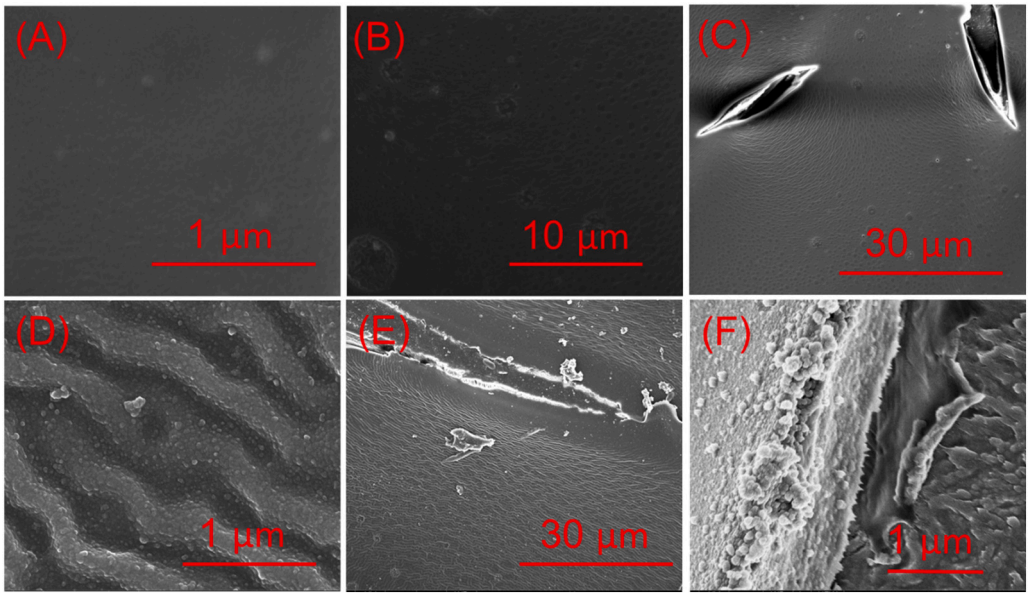

Fig. 2. SEM images of a bare (A, B & C), and $(PSS/PAH)_{10}PSS$-modified (D, E & F) Fujifilm anion-exchange membranes.

thickness and Cauche model was employed to fit film refractive indices, where DI H_2O was specified as ambient medium at 25 °C. Ellipsometric measurements were performed on 2 or 3 spots of each wafer. Three triplicate films on three different wafers were used for these measurements. The fitted refractive index for the swollen film was 1.460. The dry thickness of the $(PAH/PSS)_{10}PAH$ film assembled on Au-coated wafer was found to be of 620 ± 6 Å, whereas thickness of the film in 0.01 M solution with respect to each NaCl and Na_2SO_4 was found to be 945 ± 7 Å.

We estimated the ion permeability coefficients in the $(PSS/PAH)_{10}PSS$ films by depositing these films on porous alumina substrate. The diffusion dialysis fluxes of ions through these membranes depend on both the alumina substrate and the coating. Eq. (2) [46,47] describes the flux of salt, j, through each region of these composite membranes.

$$j = P\Delta C \tag{2}$$

where ΔC is the concentration difference across the membrane and P is the local permeance. Eq. 3 [46] describes the film permeance, P_{film}. In Eq. (3), $P_{composite}$, is the permeance of the coated alumina membrane and $P_{support}$ is the permeance of the bare membrane.

$$P_{film} = \frac{P_{composite}P_{support}}{P_{support} - P_{composite}} \tag{3}$$

We used Eq. (2) to determine the values of $P_{composite}$ and $P_{support}$ for sodium chloride and sodium sulfate. Next we employed Eq. (3) to estimate the values of P_{film} for NaCl and Na_2SO_4. The P_{film} values for NaCl and Na_2SO_4 were found to be 5.12 μm/s and 1.24 μm/s respectively. Then, we used salt permeance values in eq. 4 to determine the ion permeance coefficients. Eq. (4) [47] describes the P_{salt} (salt permeance) in terms of P_{cat} (cation permeance) and P_{an} (anion permeance). In this equation, z_{cat} is the charge on the cation and z_{an} is the charge on the anion.

$$P_{salt} = \frac{-z_{an}P_{an}P_{cat} + z_{cat}P_{an}P_{cat}}{z_{cat}P_{cat} - z_{an}P_{an}} \tag{4}$$

To describe P_{NaCl} and $P_{Na_2SO_4}$, Eq. (4) provides 2 separate equations in terms of P_{Cl^-}, $P_{SO_4^{2-}}$, and P_{Na^+}. We require one more independent equation to determine the values of ion permeances. Literature suggests that PAH/PSS films are selective for anions transport over cations transport. The Cl^- transference number was found to be ~0.65 through PAH/PSS films, whereas K^+ transference number was ~0.35. The same behavior was assumed for Na^+ and Cl^- to obtain another independent equation to estimate the P_{Cl^-}, $P_{SO_4^{2-}}$, and P_{Na^+} values.

We calculated the ion permeability coefficients of 2.44×10^{-11} dm^2/s for Cl^-, 1.71×10^{-12} dm^2/s for SO_4^{2-}, and 1.22×10^{-11} dm^2/s for Na^+ ions. We used Na_2CO_3 as an eluent in ion chromatography and thus we could not determine its permeability coefficients. However, we can assume that permeability coefficient of CO_3^{2-} will approximately be the same as that of SO_4^2 ions. Literature [48] suggests the values of diffusion coefficients of 4.61×10^{-8}, 2.43×10^{-8}, 2.18×10^{-8}, and 3.02×10^{-8} dm^2/s for Cl^-, SO_4^{2-}, CO_3^{2-}, and Na^+ ions respectively in the anion-exchange membranes.

3.3. Current-voltage (I-V) curves

The values of limiting currents for the AEMs coated with different PAH/PSS-films were measured by employing current-voltage curves method. An estimation of I_{lim} values is important to perform a current efficient separation of ions in electrodialysis. A four-point approach was opted to measure current-voltage curves in an electrochemical cell. To establish a constant current across the membrane, a potential was provided to the Pt electrodes dipped into the receiving and source phases. At the same time, both phases were aggressively swirled to lessen concentration polarization. To reduce the voltage drop across the solution between the AEMs and the reference electrode, the Haber-Luggin capillaries were kept within 4 mm of the AEM's surface. At current densities increasing from 0 to 4.7 mA cm^{-2}, the voltage drop across the unmodified and modified membranes was calculated using the electrical potential difference between the reference electrodes. For these measurements, 0.01 M NaCl and 0.1 M Na_2SO_4 were present in both the source and the receiving phases. The high concentration of multivalent anions is needed to decrease the solution resistance and to accurately measure the transmembrane potential. Over the course of *I-V* measurements, the pH of the source phase changed from ~6.6 to ~10.7 and the receiving phase pH decreased from ~6.6 to ~3.

The limiting current can be estimated using *I-V* curves. Three zones make up a typical *I-V* curve, as indicated in the Fig. 8. The potential drop across an IEM in the ohmic zone rises linearly at low current density values. However, the voltage drop across an IEM increases rapidly when current density values increase beyond the limiting current density to form a "plateau area". An overlimiting area eventually develops at even higher values of current density, where several phenomena, including

electro-convection and water splitting, cause the current to grow. An estimate of the limiting current can be obtained from the junction of the lines designating the ohmic and plateau regions.

Fig. 3 shows *I-V* curves for a bare membrane and $(PSS/PAH)_{10}PSS$- and $(PSS/PAH)_{11}$-coated AEMs. In these studies, the solutions contained 0.01 M NaCl and 0.1 M Na_2SO_4 in both the receiving and the source phases. The high SO_4^{2-} concentration minimizes the solution resistance to allow an accurate measurement of the transmembrane potential difference, but if the membrane is not highly selective SO_4^{2-} passage may increase the limiting current. This is a major limitation of these experiments because in ED experiments with a current density of 0.63 mA cm^{-2}, the ratios of Cl^- and SO_4^{2-} fluxes were only 2. Moreover, this ratio may decline further at higher current densities. Thus, the limiting currents likely represent the sum of Cl^- and SO_4^{2-} transport. Unfortunately, lower SO_4^{2-} concentrations in the solutions lead to unacceptably high potential drops.

The *I-V* curves for AEMs coated with $(PSS/PAH)_{10}PSS$ on both sides or on the cathode side exhibit distinguishable ohmic, plateau and overlimiting regions, with a limiting current density of 1.7–1.8 mA cm^{-2}. The overlimiting region is not as distinct for the $(PSS/PAH)_{11}$-coated membrane, but the limiting current density is around 2 mA cm^{-2}. For the same current density, the potential drop across $(PSS/PAH)_{11}$-coated membranes is marginally lower than the potential drop across $(PSS/PAH)_{10}PSS$ membranes, presumably because termination with a polycation leads to less electrostatic exclusion of anions. Again, we emphasize that the limiting current includes a large contribution from SO_4^{2-} transport.

Fig. 3 also shows the *I-V* curves for AEMs modified with $(PSS/PAH)_{10}PSS$ films on either their anode-facing or cathode-facing side. Bare membranes and the modified membrane with the film on the anode side behave similarly showing only ohmic regions. In contrast, the membrane with $(PSS/PAH)_{10}PSS$ on the cathode side shows ohmic, plateau and overlimiting regions similar to those of an AEM coated on both sides. When the film faces the anodic phase, accumulation should occur at the AEM-PEM interface and the limiting current due to concentration polarization at the source-phase/AEM interface is likely higher than 4 mA cm^{-2}.

We measured resistance of the bare AEM using the same approach where a plot between the applied current density and the voltage drop across the AEM was obtained. For this purpose, we employed 0.01 M NaCl and 0.1 M Na_2SO_4 both in the source and receiving phases. The resistance of the solution was measured separately and the resistance of the bare membrane was measured by subtracting the resistance of solution from the obtained combined resistance of solution and membrane. Conductance of the membrane was measured by taking the reciprocal of the membrane's resistance which was $0.056 \pm 0.005\ \Omega^{-1}$.

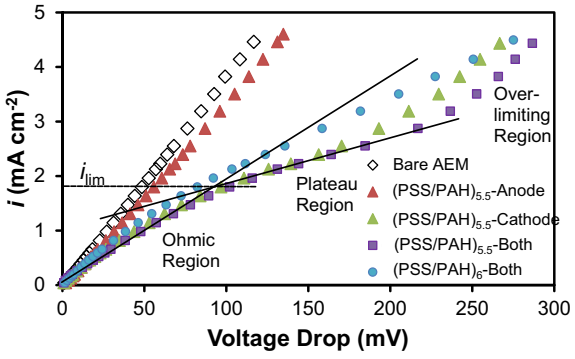

Fig. 3. *I-V* curves for ED through membrane modified with different polyelectrolyte coatings on either or both sides of the membrane. These experiments employed a 2-compartment cell with 0.01 M NaCl and 0.1 M Na_2SO_4 on both sides of the AEM. The high concentration of Na_2SO_4 decreases the solution resistance. Similar data were obtained with replicate membranes.

3.4. Electrodialysis and diffusion dialysis with bare and modified anion-exchange membranes

After estimating the values of I_{lim} through *I-V* curves, we used the coated AEMs in electrodialysis and diffusion dialysis experiments to yield a selective transport of anions. Deposition of $(PSS/PAH)_{10}PSS$-films on Fujifilm anion-exchange membranes yields an impressive increase in electrodialysis selectivity for Cl^- over SO_4^{2-} ions. Fig. 4 depicts the total moles of Cl^- and SO_4^{2-} in the receiving phase versus time during 120 min of ED from a source phase which contained 0.01 M NaCl and 0.01 M Na_2SO_4. Bare membranes show high passages of both Cl^- and SO_4^{2-} ions and the average Cl^-/SO_4^{2-}selectivity of the unmodified membrane was only 1.3. However, after modifying Fujifilm AEMs with $(PSS/PAH)_{10}PSS$ films on both sides, the SO_4^{2-} flux decreases to nearly undetectable levels and the Cl^- flux increases, giving rise to a remarkable Cl^-/SO_4^{2-} selectivity of around 180. This value is much greater than the typical selectivities of AEMs [49–51] and indicates that polyelectrolyte films fully cover the surface and channels in Fujifilm membranes. Thus, PEMs deposited on an AEM act as a selective barrier. Increasing the number of bilayers increases the thickness of the film and the selectivity of monovalent to divalent ions through a membrane [36]. However, increased thickness of the film slows down the electrodialysis process and hence the recovery of the ions of interest. We found the thickness of 10.5 bilayers of PSS and PAH polyelectrolyte as optimum to give us a reasonable flux and a remarkable selectivity through the membranes. As Table 1 and Fig. 4 show, the ED Cl^- flux through the modified membranes increases on average 43 % compared to the bare membranes because Cl^- ions carry a major portion of the current in the coated system.

We also performed DD using the same 3-compartment cell and solutions as in ED but without applying any current. For unmodified membranes, the Cl^- fluxes in DD were about 20 % lower than those in ED (Table 1), and the Cl^-/SO_4^{2-} selectivity was 1.7. The $(PSS/PAH)_{10}PSS$-modified membranes showed a 70 % decline in Cl^- flux on going from ED to DD, but the SO_4^{2-} flux decreased even more to give a Cl^-/SO_4^{2-} selectivity >280. The $(PSS/PAH)_{10}PSS$ film clearly provides a barrier that decreases diffusive flux compared to a bare membrane, but the barrier is selective for Cl^- over SO_4^{2-}.

The DD fluxes through the $(PSS/PAH)_{10}PSS$-coated AEMs are higher than one might expect because Cl^- and SO_4^{2-} diffusion from a source to a receiving phase requires either counter diffusion of CO_3^{2-} or co-diffusion of Na^+ through the AEMs. For the bare membrane, counter diffusion of CO_3^{2-} may readily occur, but we would expect the coated membranes to resist passage of all divalent anions. Below we discuss the mechanisms for maintaining electrical neutrality in more detail.

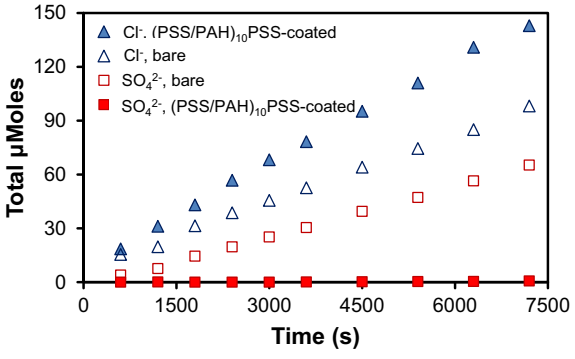

Fig. 4. Total µMoles of Cl^- (triangles) and SO_4^{2-} (squares) in the receiving compartment versus time when source phase contained 0.01 M with respect to each NaCl and Na_2SO_4 during electrodialysis. The open and filled symbols show ED (current density = 0.63 mA cm^{-2}) through bare and $(PSS/PAH)_{10}PSS$-coated AEMs, respectively. A 0.01 M Na_2CO_3 solution was used initially in the receiving and isolated anodic compartments.

Table 1
Cl^- and SO_4^{2-} fluxes and Cl^- to SO_4^{2-} selectivities during DD and ED through coated and bare Fujifilm AEMs. 0.01 M Na_2CO_3 was used as a receiving phase initially, the source phase was 0.01 M with respect to each NaCl and Na_2SO_4, and 0.63 mA cm^{-2} was the current density. The current efficiencies were calculated in terms of transference numbers in ED which are listed in parentheses.

	Fujifilm membrane	Cl^- flux (nmol cm^{-2} s^{-1})	SO_4^{2-} flux (nmol cm^{-2} s^{-1})	Selectivity
ED	$(PSS/PAH)_{10}PSS$-coated	5.94 ± 0.13 (0.90 ± 0.02)	0.036 ± 0.009 (0.011 ± 0.003)	180 ± 60
	Bare	4.15 ± 0.18 (0.63 ± 0.02)	3.13 ± 0.14 (0.95 ± 0.04)	1.33 ± 0.01
DD	$(PSS/PAH)_{10}PSS$-coated	1.81 ± 0.22	<0.0067	>244
	Bare	3.44 ± 0.06	2.08 ± 0.12	1.66 ± 0.07
ED	$(PSS/PAH)_{11}$-coated	4.65 ± 0.34 (0.70 ± 0.05)	0.467 ± 0.120 (0.141 ± 0.036)	10 ± 3
DD	$(PSS/PAH)_{11}$-coated	1.80 ± 0.14	0.096 ± 0.032	21 ± 6

As Fig. 4 shows, the total μmoles of Cl^- and SO_4^{2-} ions in the source phase increase essentially linearly versus time. A small decrease in Cl^- flux near the end of 2 h of ED might occur and stem from an increase in the amount of OH^- in the source phase (cathodic compartment). Over the course of ED, the pH of the source phase goes up from 6.5 to 10.9 (coated membranes) and from 6.5 to 11.1 (bare membranes), whereas the receiving phase pH goes a little down from 11.3 to 11.1 (for both bare and modified membranes). A 0.01 M solution of Na_2CO_3 in the receiving and isolated anode compartments resists the significant pH change that should result from formation of protons at the anode. During ED, the pH of the isolated phase decreases more (from 11.3 to 10.7) than the pH of the receiving phase. In DD, the amounts of Cl^- and SO_4^{2-} increase linearly with time due to the low receiving-phase concentrations of these ions and, hence, a constant concentration gradient across the membrane.

To examine whether selectivity depends on the composition of the terminating polyelectrolyte layer, we also determined the selectivities of membranes coated with $(PSS/PAH)_{11}$ films, which terminate in a polycation (PAH). Fig. 5 demonstrates the total moles of Cl^- and SO_4^{2-} that permeated through the membrane during 2 h of DD or ED. Over the first 30 min of ED, the Cl^- flux was about 9.80 ± 0.38 nmol cm^{-2} s^{-1}, but then it decreased significantly to 4.65 ± 0.34 nmol cm^{-2} s^{-1} during the remaining 1.5 h of dialysis. The SO_4^{2-} flux increased to 0.467 ± 0.120 nmol cm^{-2} s^{-1} after 30 min giving rise to a selectivity of 10 ± 3 in ED. We think that SO_4^{2-} adsorption into these polycation-terminated films

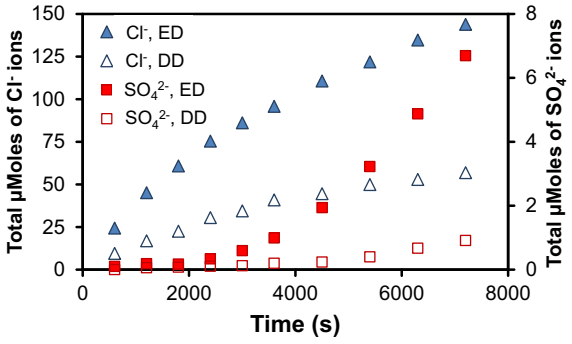

Fig. 5. Total μMoles of Cl^- (triangles) and SO_4^{2-} (squares) in the receiving phase versus time during 2 h ED and DD. The source phase was 0.01 M with respect to each NaCl and Na_2SO_4 whereas each of receiving and isolated anode compartments contained 0.01 M Na_2CO_3 as initial solutions. The open symbols represent DD and filled symbols represent ED through $(PSS/PAH)_{11}$ modified AEMs. In ED, 0.63 mA cm^{-2} was the applied current density. Note the different scales for Cl^- and SO_4^{2-} flux.

increases films swelling to decrease selectivity. The Cl^- flux declines because SO_4^{2-} carries a larger fraction of the current. We performed another 2 h of ED with the same membranes after rinsing the cells with DI H_2O and refilling them with new solutions. For the second 2 h of ED, plots similar to Fig. 5 showed linear trends over the entire time. The Cl^- flux decreased to 4.4 nmol cm^{-2} s^{-1} while the SO_4^{2-} flux increased to 0.67 nmol cm^{-2} s^{-1} to give a Cl^-/SO_4^{2-} selectivity of ~7. In DD, the Cl^- flux was 4.56 ± 0.98 nmol cm^{-2} s^{-1} during the first 30 min and then decreased significantly to 1.80 ± 0.14 nmol cm^{-2} s^{-1} during remaining 90 min which again in part be due to an increase in the SO_4^{2-} flux after 30 min of diffusion dialysis.

To measure the Cl^-/SO_4^{2-} selectivity, we used AEM between the central and the cathodic compartment to transport our ions of interest from the source (cathodic) to the receiving (central) phase. We inserted a bare CEM between the central and the anodic compartment to block the passage of Cl^- to the anodic compartment and hence to avoid the oxidation of Cl^- ions into Cl_2 gas on the anode. Conversion of Cl^- into Cl_2 could alter our results. Also, literature suggests that Cl_2 gas can potentially destroy the deposited PEMs on the IEMs. Therefore, it was important to isolate the anodic compartment from the receiving phase by inserting a standard CEM. It is important to note that OH^- ions are produced due to the reduction of water on the cathode, which may carry current across the AEM (in addition to our anions of interest) to decrease the current efficiency. At 2 mA cm^{-2} applied current density, the concentration of OH^- ions in the source phase at the end of 2 h ED is only 0.0017 M which is much lower as compared to the concentrations of Cl^- in the source phase. We used a four compartments cell to avoid the transport of OH^- across an AEM, where we isolated the source phase from the cathodic compartment by inserting a CEM between them but the pH of the source and the cathodic was not found much different from each other. The OH^- ions are highly mobile and the applied electric potential favors their movement from cathodic compartment to the source phase. Also when we used 0.005 M or 0.01 M concentrations with respect to each NaCl and Na_2SO_4 in the source phase, the electrical resistance of the four compartments ED setup increased unacceptably and we were unable to generate higher current densities to study the transport phenomenon in the overlimiting zone. Keeping in view all these factors, we used 3-compartment electrodialysis setup and performed the ED experiment for 2 h to keep the concentration of OH^- ions lower in the source phase. Unfortunately, there would be a small portion of the current being carried by OH^- ions especially near the end of 2 h ED.

We used sodium carbonate solution as the receiving phase because in ion chromatography the suppresser suppresses the concentration of carbonate ions and we do not get any additional peak in the ion chromatograph due to them. However, we could get giant peaks in ion chromatographs if we employ some other salt solutions (such as $NaNO_3$, Na_3PO_4, Na_2SO_4 etc.) as the receiving phase which may interfere with the peaks of our ions of interest and hence with the accuracy of our results. We used sodium carbonate in the anodic compartment as well instead of some other salts (such as $NaNO_3$, Na_2SO_4 etc.) because our CEMs are not 100 % selective for cations over anions and diffusion of SO_4^{2-} ions from anodic compartment to the receiving phase could alter our results. Moreover, Na_2CO_3 acts as a buffer to resist a change in the pH of the anodic compartment due to the production of H^+ ions on the anode.

To measure the stability of coating at a wider range of pH, we kept our coated membranes in 0.5 M NaOH solution overnight and then performed the ED through them. The ED results (in terms of fluxes of ions and selectivities) were not different from those obtained through coated membranes which were not kept in 0.5 M NaOH solutions overnight. Similarly, we kept our coated AEMs in 0.5 M HCl solutions overnight prior to using them in ED. Again the results were not found different. This shows that the membranes are stable at a wider range of pH.

3.5. Selectivities of membranes coated on one side

One-sided coated membranes (rather than coated on both sides) may show less resistance to mass transport. Thus, we examined the DD and ED fluxes of targeted anions through one-sided coated AEMs where coating either faced the anode or the cathode. Table 2 compares ED and DD ion fluxes and Cl^-/SO_4^{2-} selectivities for bare and several membranes modified on only one side. With $(PSS/PAH)_{10}PSS$ films and comparison of the one-side and two-side coated membranes, the ED and DD selectivity is at least an order of magnitude higher for films coated on both faces. Moreover, for single-side coated membranes, the ED selectivity with the coating facing the cathode (equivalently facing the receiving phase) is double that when the coating faced the anode. In some previous work with cation transport through modified CEMs, a similar trend where the K^+/Mg^{2+} selectivity was higher with the coating facing the anode was reported [9]. This effect likely stems from concentration polarization at the AEM-coating interface when the coating faces the receiving phase in ED (Fig. 6). Inside the AEM anions are the primary current carriers, but both the monovalent ion and Na^+ carry current through the $(PSS/PAH)_{10}PSS$ film. Thus, the anion and cation concentrations, especially the divalent ions, will increase near the membrane/film interface. When the membrane faces the source phase, sulfate will accumulate at the surface of the $(PSS/PAH)_{10}PSS$ film, but high diffusion coefficients in solution will help mitigate this concentration polarization.

In all cases, the Cl^- and SO_4^{2-} fluxes are lower in DD than in ED. However, the Cl^-/SO_4^{2-} selectivity trends among the different membranes listed in Table 2 are different for ED and DD. In particular, in DD selectivity for single-side coated membranes is higher when PEMs faced the receiving phase. The $(PSS/PAH)_{10}PSS$ film may become more selective due to lower ion chemical potentials at the membrane-film interface compared to at the solution-film interface when PEMs faced the source phase.

3.6. Estimation of current efficiencies

High current efficiencies are important for creating energy-efficient ED separations. However, determining current efficiencies in the three-cell setup is difficult due to the presence of both diffusive and electromigration transport. Moreover, the non-electrical transport involves coupled ion diffusion. One could simply subtract the DD flux from the ED flux to try to calculate transport due to electromigration, but the electrically coupled ion diffusion may change significantly due to the applied electrical potentials in ED.

To better understand the electrically coupled diffusion, we replaced the 0.01 M NaCl, 0.01 M Na_2SO_4 source phase with 0.01 M KCl, 0.01 M K_2SO_4 so we could determine whether there is significant cation movement from the receiving to the source phase and vice versa. In DD, the flux of K^+ permeating to the receiving phase was 0.191 ± 0.032 nmol cm^{-2} s^{-1}, whereas the flux of Cl^- permeating to the receiving phase was 1.76 ± 0.21 nmol cm^{-2} s^{-1}. The co-diffusion of K^+ and Cl^- would account for only 12 % of the Cl^- diffusive flux. Unfortunately due to the use of CO_3^{2-} as an eluent in ion chromatography, we could not measure the CO_3^{2-} flux to the source phase. However, ICP analysis indicated an undetectable Na^+ concentration in the source phase, ruling out significant co-diffusion of CO_3^{2-} and Na^+ to the source phase or counter-diffusion of Na^+ and K^+. During 2 h of DD, the source-phase pH increased from 6.5 to 10.2 while the receiving phase pH decreased from 11.4 to 10.7. These pH changes suggest coupled counter-diffusion of Cl^- with OH^- or CO_3^{2-}. Because CO_3^{2-} is divalent, we suspect the coupled diffusion primarily occurs with OH^-. We performed DD experiments to understand of co-diffusion of cations and counter diffusion of anions through AEMs.

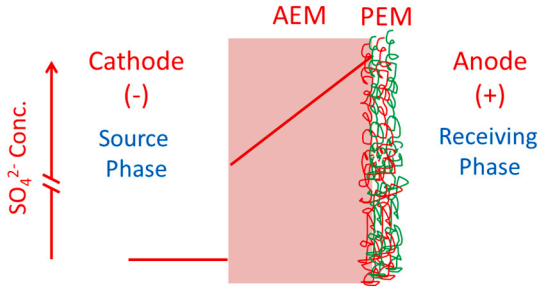

Fig. 6. A schematic diagram qualitatively showing the SO_4^{2-} concentration profile (red lines) during ED through an AEM with coating facing the receiving phase. The SO_4^{2-} concentration builds up in AEM under applied current because of its lower permeability through PEM and lower diffusion in AEM.

In ED with 0.01 M KCl, 0.01 M K_2SO_4 as the source phase and $(PSS/PAH)_{10}PSS$-coated membranes (both sides), the flux of K^+ to the receiving phase was only 0.029 ± 0.006 nmol cm^{-2} s^{-1}, consistent with the applied potential decreasing cation transport to the source phase. Similarly, the flux of CO_3^{2-} or OH^- to the source phase should also decrease in ED compared to DD to reduce coupled anion counter-diffusion. When we used 0.03 M $NaHCO_3$ in the receiving phase, the chloride flux was 3.82 nmol cm^{-2} s^{-1} in DD which is ~2 times greater than the DD Cl^- flux with 0.01 M Na_2CO_3 in the receiving compartment, indicating higher counter-diffusion of Cl^- with HCO_3^- compared to with CO_3^{2-}. In contrast Cl^- flux (5.92 nmol cm^{-2} s^{-1}) in ED was about the same when using 0.03 M $NaHCO_3$ or 0.01 M Na_2CO_3 in the receiving phase. Also, for both ED and DD, the Cl^-/SO_4^{2-} selectivity did not change significantly while using either 0.03 M $NaHCO_3$ or 0.01 M Na_2CO_3 in the receiving and isolated phases. Thus, for coated membranes transference number calculated based on ion analyses are likely reasonable estimates. This is not the case for bare membranes.

Table 1 gives values of Cl^- transference numbers for several different membranes. These values do not correct for possible diffusive flux, so for bare membranes the sum of the transference numbers may exceed unity. Membranes coated on both sides with $(PSS/PAH)_{10}PSS$ films show an impressive Cl^- transference number of ~0.9. For membranes modified with $(PSS/PAH)_{11}$ films, the transference number is only 0.70 ± 0.05. Much of the remaining transference stems from SO_4^{2-}. The uncorrected Cl^- transference numbers of membranes coated with $(PSS/PAH)_{10}PSS$ only on one side are also <1, primarily because sulfate carries a large portion of the current. For AEMs coated with $(PSS/PAH)_{10}PSS$ only on the anode side, the sum of the SO_4^{2-} and Cl^- transference numbers is >1, showing that this system clearly needs some correction for diffusive flux. When the sums of transference numbers for Cl^- and SO_4^{2-} are significantly <1, water splitting may account for the extra current [36,52]. Please note that the current efficiencies are measured in terms of transference number, which is portion of the current being carried by a given ion in electrodialysis.

Table 2
Cl^- and SO_4^{2-} fluxes and Cl^- to SO_4^{2-} selectivities during ED and DD through Fujifilm AEMs coated with $(PSS/PAH)_{10}PSS$-films. The source phase was 0.01 M with respect to each NaCl and Na_2SO_4, the receiving and isolated phases initially were 0.01 M Na_2CO_3 solutions, and 0.63 mA cm^{-2} was the applied current density in ED. The current efficiencies measured in terms of transference numbers for ED are listed in parentheses.

	Coating facing	Cl^- Flux (nmol cm^{-2} s^{-1})	SO_4^{2-} Flux (pmol cm^{-2} s^{-1})	Selectivity
ED	Source phase	4.78 ± 0.35 (0.72 ± 0.06)	562.6 ± 80.1 (0.167 ± 0.025)	8.6 ± 0.6
	Receiving phase	5.55 ± 0.39 (0.84 ± 0.06)	1518.1 ± 202.2 (0.457 ± 0.064)	3.7 ± 0.2
DD	Source phase	2.02 ± 0.22	226.98 ± 18.4	8.9 ± 0.6
	Receiving phase	2.85 ± 0.26	161.1 ± 45.3	18.2 ± 3.2

3.7. Effect of current density on Cl^-/SO_4^{2-} separations

ED induces a depletion layer at the interface between the cathode-facing PEM and the AEM because the anion transference numbers are higher in the AEM than in the PEM coating (see Fig. 6). Because the anions carry a larger portion of current in the AEM than in the PEM, both the anion and cation concentrations decrease at the PEM-AEM interface [20]. Steady-state transport in this region requires diffusion of anions and cations to the interface. However, as the interfacial concentrations approach zero, a limiting current appears because the diffusive flux to the interface reaches its maximum value. Eq. (5) [20] gives an estimate of the limiting current density, I_{lim}

$$I_{lim} = \frac{P_s x c x F}{\triangle t_-} \quad (5)$$

where, P_s is diffusion salt permeance of coating, c is the concentration of a monovalent anion in the source phase, F is the Faraday constant and $\triangle t_-$ is the difference of the transference numbers of monovalent anions in the coating and the AEM. The operation of ED at and above the limiting current often leads to water splitting which is a parasitic processes, so a knowledge of the limiting current is important for energy-efficient separation. Importantly, higher limiting currents will help to increases the rate of ED or decreases the membrane area (Fig. 7).

Three areas make up a typical current-voltage (*I-V*) curve. The potential drop across the membrane in the ohmic zone rises linearly at low current density values. The voltage drop across the membranes rapidly rises with an increase in the current density over the limiting current density to form a plateau zone. At even higher values of current density, an overlimiting area eventually develops where several phenomena, including electro-convection and water splitting, cause the current to grow. Fig. 8 shows the Cl^- and SO_4^{2-} fluxes against current density in ED through AEMs coated with $(PSS/PAH)_{10}PSS$ films. The Cl^- flux shows an initial rapid increase, a plateau region, and then a more rapid increase similar to an *I-V* curve. This plot suggests a limiting current value around 0.6 mA cm^{-2}, which is similar to previous estimates of limiting currents for cation exchange membranes coated with $(PAH/PSS)_{10}PAH$ films [20]. This is also consistent with determination of film permeabilities in diffusion dialysis measurements with coated porous alumina membranes [43].

As the Cl^- flux plateaus in Fig. 8, the SO_4^{2-} flux rises rapidly. As current densities approach or exceed the limiting value, the electric field near the $(PSS/PAH)_{10}PSS/AEM$ interface should increase rapidly and may give rise to water splitting and a locally low pH [36,52]. Formation of monovalent HSO_4^- could greatly increase the sulfate flux. Previous studies show that the flux of anions through polyelectrolyte multilayers

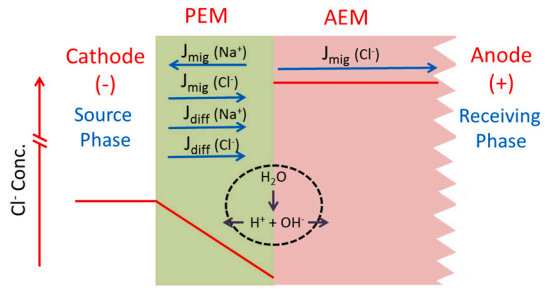

Fig. 7. A schematic diagram showing the qualitative concentration profile of Cl^- (red lines) during ED through a polyelectrolytes coated AEM. The blue arrows indicate the magnitudes of electromigration (J_{mig}) or diffusion fluxes (J_{diff}) of cations and anions qualitatively in the coating and/or AEM. The sum of J_{mig} and J_{diff} in the PEM should equal the J_{mig} in the AEM at steady state, where J_{diff} is too small as compared to J_{mig}. The amount of Cl^- may not be constant in AEM because of possible $[OH^-]$ gradients. The coating/membrane interface near the receiving phase (not shown) should indicate Cl^- accumulation instead of depletion.

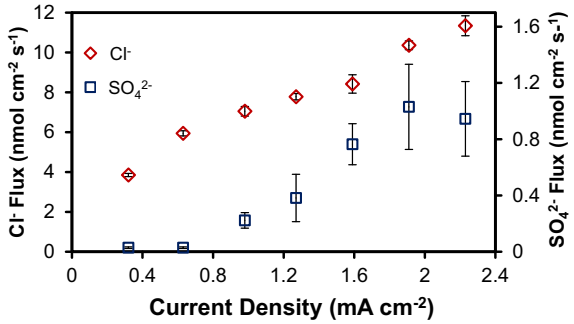

Fig. 8. Effect of applied current density on Cl^- and SO_4^{2-} fluxes in 3-compartment ED experiments with 0.01 M Na_2CO_3 in the receiving and isolated anodic phases. The AEM membrane was modified with a $(PAH/PSS)_{10}PAH$ coating. The source phase was initially 0.01 M with respect to each NaCl and Na_2SO_4. Note that the scales for Cl^- and SO_4^{2-} fluxes are different.

increases after protonation [53,54].

As expected, the Cl^- transference number decreases as the current density approaches or exceeds the limiting value (Table 3). However, in the overlimiting region, the Cl^-/SO_4^{2-} selectivity and the Cl^- transference number are approximately constant. Although operating at such high current densities is only 50 % efficient in terms of Cl^- transport, it does allow for faster separations, and the Cl^-/SO_4^{2-} selectivity is still around 10.

3.8. Electrodialysis with different source-phase concentrations

If a polyelectrolyte film's ion adsorption or charge screening have an impact on ion transport across $(PAH/PSS)_{10}PAH$ films, selectivities may differ greatly depending on the amounts of source-phase ions. Furthermore, the limiting currents will rise with an increase in the ion concentrations. We performed ED with Cl^- and SO_4^{2-} source-phase concentrations varying from 0.005 M to 0.1 M, whereas 0.01 M Na_2CO_3 was always employed as a receiving and isolated phase, and the value of current density was adjusted at 0.63 mA cm^{-2}, to examine the impact of concentrations in the source phase on selectivity and fluxes. As Fig. 8 shows, the Cl^- flux increases from 4.8 to 10.8 nmol cm^{-2} s^{-1} as the concentration in the source phase rises from 0.005 to 0.1 M for both NaCl and Na_2SO_4. The SO_4^{2-} flux, however, initially drops from 0.075 to 0.036 nmol cm^{-2} s^{-1} when the Cl^-/SO_4^{2-} concentration in the source phase rises from 0.005 to 0.010 M, suggesting that the applied current density approaches the limiting value for Cl^- only at the minimum source-phase concentration of 0.005 M. Less water splitting with 0.01 M Cl^- and SO_4^{2-} source-phase concentrations leads to less sulfate transport. The simultaneous decrease in SO_4^{2-} flux and increase in Cl^- flux lead to an increase in Cl^- to SO_4^{2-} selectivity from ~68 to ~180 (see Table 4) when the concentrations in the source-phase change from 0.005 to 0.01 M.

As the source phase concentration goes up more from 0.01 to 0.1 M, the SO_4^{2-} flux increases continuously from 0.036 to 0.220 nmol cm^{-2} s^{-1}, and the Cl^-/SO_4^{2-} selectivity decreases from ~180 to ~50. At these

Table 3
Transference number of anions and Cl^-/SO_4^{2-} selectivities in ED through $(PSS/PAH)_{10}PAH$-coated aliphatic polyamide AEMs versus current density. Initially, the source phase contained 0.01 M NaCl and 0.01 M Na_2SO_4.

i (mA cm^{-2})	Cl^- transference	SO_4^{2-} transference	Cl^-/SO_4^{2-} selectivity
0.32	1.17 ± 0.03	0.013 ± 0.001	>165
0.63	0.90 ± 0.02	0.011 ± 0.003	>144
0.98	0.71 ± 0.02	0.035 ± 0.010	42 ± 11
1.27	0.59 ± 0.01	0.058 ± 0.026	24 ± 8
1.59	0.51 ± 0.03	0.093 ± 0.018	12 ± 2
2.07	0.52 ± 0.01	0.104 ± 0.030	11 ± 3
2.23	0.49 ± 0.02	0.082 ± 0.020	13 ± 3

Table 4
Cl^-/SO_4^{2-} transference numbers and Cl^-/SO_4^{2-} selectivities in ED through $(PSS/PAH)_{10}PSS$-coated AEMs. 0.01 M Na_2CO_3 was used in each of the receiving and isolated phases. The applied current density was 0.63 mA cm^{-2}.

Source-phase Cl^-/SO_4^{2-} conc. (M)	Cl^- transference	SO_4^{2-} transference	Selectivity
0.005	0.73 ± 0.03	0.023 ± 0.006	68 ± 19
0.010	0.90 ± 0.02	0.011 ± 0.003	176 + 55
0.020	0.95 ± 0.01	0.022 ± 0.003	88 ± 14
0.050	1.19 ± 0.02	0.048 ± 0.008	50 ± 9
0.100	1.64 ± 0.20	0.066 ± 0.007	50 ± 10

higher concentrations, the ion fluxes are a combination of diffusive and electromigration transport. Decrease in the Cl^-/SO_4^{2-} selectivity at higher source phase concentrations likely stems from charge screening that decreases SO_4^{2-} ions electrostatic exclusion. Also, PEM swelling increases in solutions of higher ionic strengths [55], which may decrease selectivity. We also performed diffusion dialysis under similar conditions but with no applied current (Table 5). In DD, the Cl^- and SO_4^{2-} fluxes increase continuously when the feed concentration goes up from 0.005 to 0.1 M, but the Cl^-/SO_4^{2-} selectivity decreases at concentrations above 0.01 M. Again, charge screening at high concentrations likely leads to less electrostatic exclusion of the divalent SO_4^{2-} [56,57].

We also examined the selectivity of PEMs-coated AEMs when source-phases contained unequal concentrations of Cl^- and SO_4^{2-}. In these experiments, the applied current density was 0.63 mA cm^{-2} and the isolated and receiving phases always contained 0.01 M Na_2CO_3. When the source phase was 0.01 M with respect to each NaCl and Na_2SO_4, the Cl^- and SO_4^{2-} fluxes were 3.54 ± 0.14 and 1.83 ± 0.05 nmol cm^{-2} s^{-1} respectively, producing a Cl^-/SO_4^{2-} flux ratio of 1.93 ± 0.08. However, if we consider the SO_4^{2-} to Cl^- concentration ratio of 10 in the source phase, the actual selectivity in this separation is 19.3 ± 0.8. We performed DD under similar conditions to find the fluxes and Cl^-/SO_4^{2-}selectivity without an applied current. The Cl^- and SO_4^{2-} diffusive fluxes were 1.80 ± 0.04 and 0.60 ± 0.08 nmol cm^{-2} s^{-1} respectively in DD, giving rise to a Cl^-/SO_4^{2-} flux ratio of 3.00 ± 0.35 and a Cl^-/SO_4^{2-} selectivity of 30.0 ± 3.5. A higher selectivity in DD than in ED suggests that water splitting in ED may produce HSO_4^- locally to increase transport of sulfate species. This may also help to understand why the Cl^- to SO_4^{2-} ED selectivity is lower for source phases having 0.01 M Cl^- and 0.1 M SO_4^{2-} compared to solutions containing 0.1 M concentrations of both ions. In the reciprocal experiment, when the source phase contained 0.1 M NaCl and 0.01 M Na_2SO_4, the Cl^- and SO_4^{2-} fluxes were 13.00 ± 0.12 nmol cm^{-2} s^{-1} and < 0.0013 nmol cm^{-2} s^{-1}, respectively giving a Cl^-/SO_4^{2-} flux ratio of >920 in ED. The Cl^- transport number was 1.97 ± 0.01 indicating a large contribution of Cl^- diffusion to the total flux.

3.9. Electrodialysis with a 2-compartment cell

To investigate the effect of having the anode in direct contact with the Cl^- in the receiving phase, we performed ED in a 2-compartment cell, where we used 0.01 M NaCl and 0.01 M Na_2SO_4 in the source phase and 0.01 M Na_2CO_3 solution as the receiving phase. The applied current density was 0.63 mA cm^{-2} across a $(PSS/PAH)_{10}PSS$ coated Fujifilm AEM. Compared to the 3-compartment ED as explained above, the Cl^- flux decreased from 5.90 ± 0.13 to 4.51 ± 0.22 nmol cm^{-2} s^{-1}, and the SO_4^{2-} flux remained <27 pmol cm^{-2} s^{-1} yielding a selectivity of >164. The lower Cl^- flux in 2-cell ED may partly result from oxidation of Cl^- into Cl_2 at the anode. Another possible reason for a lower Cl^- flux in 2-cell ED than in 3-cell ED could be a different pH gradient across the AEM in the two systems. In 3-cell ED, the pH values in the source phase and receiving phase after 2 h of dialysis were 11.1 and 10.9, respectively. (At the start of the experiments the pH values were 11.3 and ~ 7 in the receiving and source phases, respectively.) In 2-cell ED, the pH of the receiving phase and source phase was 10.50 and 10.71, respectively, at the end of the dialysis. The higher pH with the 3-compartment cell may increase film permeability. We also performed DD in the same 2-compartment system without an applied current and the Cl^- and SO_4^{2-} fluxes were 1.90 ± 0.13 nmol cm^{-2} s^{-1} and 7.42 ± 3.01 pmol cm^{-2} s^{-1}, which are not significantly different from the diffusive fluxes of ions in a 3-compartment DD (see Table 1).

Table 5
Cl^- and SO_4^{2-} fluxes and Cl^- to SO_4^{2-} selectivities in DD through $(PSS/PAH)_{10}PSS$ modified Fujifilm AEM. 0.01 M Na_2CO_3 was used in each of the receiving and isolated phases.

Source-phase Cl^-/SO_4^{2-} conc. (M)	Cl^- flux (nmol cm^{-2} s^{-1})	SO_4^{2-} flux (pmol cm^{-2} s^{-1})	Selectivity
0.005	1.62 ± 0.06	<6.37	>265
0.010	1.81 ± 0.22	<6.69	>244
0.020	2.30 ± 0.29	18.1 ± 6.7	135 ± 35
0.050	3.44 ± 0.14	42 ± 10	84 ± 22
0.100	6.6 ± 1.4	62 ± 19	109 ± 19

4. Conclusion

Layer-by-layer addition of polyelectrolyte multilayers likely covers and modifies the entire surface of Fujifilm AEMs. Coated AEMs yield a Cl^-/SO_4^{2-} selective transport in diffusion and electrodialysis. The increase in Cl^-/SO_4^{2-} selectivity depends on the source phase salt concentrations and the applied current density. As the concentrations of salts increase from 0.005 to 0.1 M with respect to each NaCl and Na_2SO_4 in the source phase, the Cl^-/SO_4^{2-} selectivity decreases from 180 to 50 in ED. Likewise with an increase in the current density from 0.32 to 2.23 mA cm^{-2}, the Cl^-/SO_4^{2-} selectivity decreases from >165 to 13 ± 3 for a source phase containing 0.01 M of each NaCl and Na_2SO_4. In addition, a decrease in current efficiency was also noted with an increase in the current density. Current density-voltage curves indicate that when the current density values increase than 1.7 mA cm^{-2}, the phenomenon of water splitting appears and hence the value of current efficiency decreases. Moreover, the ED results obtained for the AEM coated only on the source phase were different from those obtained for the membranes coated only on the receiving side. The presence of PEMs on the source phase yielded a higher selectivity in ED, whereas the presence of coating on the receiving side produced higher selectivity in DD. These permselective AEMs can be combined with permselective CEMs in ED to separate and purify salt mixtures.

CRediT authorship contribution statement

Muhammad Ahmad: Supervision, Methodology, Formal analysis, Writing - original draft Mahmood Ahmed: Review & editing, Writing - original draft, Shabbir Hussain: Review, Analysis, Abid Ali: Review, Manzar Zahra: Review & editing, Muhammad Imran Din: Validation, Zeeshan Mustafa: Review & editing.

Informed consent

Not applicable.

Funding

There has been no financial support for this work that could have influenced its outcome.

Declaration of competing interest

We wish to confirm that there are no known conflicts of interest associated with this publication.

Data availability

No data was used for the research described in the article.

References

[1] R. Tan, A. Wang, R. Malpass-Evans, R. Williams, E.W. Zhao, T. Liu, C. Ye, X. Zhou, B.P. Darwich, Z. Fan, Hydrophilic microporous membranes for selective ion separation and flow-battery energy storage, Nat. Mater. 19 (2020) 195–202.

[2] J. Hu, X. Tang, Q. Dai, Z. Liu, H. Zhang, A. Zheng, Z. Yuan, X. Li, Layered double hydroxide membrane with high hydroxide conductivity and ion selectivity for energy storage device, Nat. Commun. 12 (2021) 1–10.

[3] D.R. McAlister, H. Kurosaki, S. Happel, E.P. Horwitz, Development of extraction chromatography resins for metal ion separations in analytical radiochemistry, Bunseki 2020 (2020).

[4] P.K. Dasgupta, F. Maleki, Ion exchange membranes in ion chromatography and related applications, Talanta 204 (2019) 89–137.

[5] M. Ahmad, Selective Ion Dialysis through Ion-Exchange Membranes Coated with Polyelectrolyte Multilayers, University Of Notre Dame, 2020.

[6] M. Ahmad, S. Hussain, M.A. Abid, A. Mumtaz, M. Ibrar, S. Muhammad, Creating bipolar junction by depositing ultrathin anion-exchange coating on cation-exchange membrane to dissociate water in electrodialysis, J. Membr. Sci. Res. 8 (2022) -.

[7] M. Ahmad, C. Tang, L. Yang, A. Yaroshchuk, M.L. Bruening, Layer-by-layer modification of aliphatic polyamide anion-exchange membranes to increase Cl−/SO42− selectivity, J. Membr. Sci. 578 (2019) 209–219.

[8] M. Ahmad, A. Yaroshchuk, M.L. Bruening, Moderate pH changes alter the fluxes, selectivities and limiting currents in ion transport through polyelectrolyte multilayers deposited on membranes, J. Membr. Sci. 616 (2020), 118570.

[9] Y. Zhu, M. Ahmad, L. Yang, M. Misovich, A. Yaroshchuk, M.L. Bruening, Adsorption of polyelectrolyte multilayers imparts high monovalent/divalent cation selectivity to aliphatic polyamide cation-exchange membranes, J. Membr. Sci. 537 (2017) 177–185.

[10] L. Yang, C. Tang, M. Ahmad, A. Yaroshchuk, M.L. Bruening, High selectivities among monovalent cations in dialysis through cation-exchange membranes coated with polyelectrolyte multilayers, ACS Appl. Mater. Interfaces 10 (2018) 44134–44143.

[11] P. Sosa-Fernandez, J. Post, F. Leermakers, H. Rijnaarts, H. Bruning, Removal of divalent ions from viscous polymer-flooding produced water and seawater via electrodialysis, J. Membr. Sci. 589 (2019), 117251.

[12] H. Lu, W. Zou, P. Chai, J. Wang, L. Bazinet, Feasibility of antibiotic and sulfate ions separation from wastewater using electrodialysis with ultrafiltration membrane, J. Clean. Prod. 112 (2016) 3097–3105.

[13] X. Wei, Y. Wang, H. Yan, K. Wu, T. Xu, Purification of methylsulfonylmethane from mixtures containing salt by conventional electrodialysis, Membranes 10 (2020) 23.

[14] E. Schreiber, R.E. Garwick, M.J. Baran, M.A. Baird, B.A. Helms, E.M. Matson, Molecular engineering of polyoxovanadate-alkoxide clusters and microporous polymer membranes to prevent crossover in redox-flow batteries, ACS Appl. Mater. Interfaces 14 (20) (2022) 22965–22972.

[15] N. Kim, J. Jeon, R. Chen, X. Su, Electrochemical separation of organic acids and proteins for food and biomanufacturing, Chem. Eng. Res. Des. 178 (2022) 267–288.

[16] Y. Xu, S. Xiang, H. Zhou, G. Wang, H. Zhang, H. Zhao, Intrinsic pseudocapacitive affinity in manganese spinel ferrite nanospheres for high-performance selective capacitive removal of Ca2+ and Mg2+, ACS Appl. Mater. Interfaces 13 (2021) 38886–38896.

[17] B. Yuzer, M.I. Aydin, H. Yildiz, B. Hasançebi, H. Selcuk, Y. Kadmi, Optimal performance of electrodialysis process for the recovery of acid wastes in wastewater: practicing circular economy in aluminum finishing industry, Chem. Eng. J. 434 (2022), 134755.

[18] J. Yan, H. Wang, R. Fu, R. Fu, R. Li, B. Chen, C. Jiang, L. Ge, Z. Liu, Y. Wang, Ion exchange membranes for acid recovery: diffusion dialysis (DD) or selective electrodialysis (SED)? Desalination 531 (2022), 115690.

[19] N. White, M. Misovich, E. Alemayehu, A. Yaroshchuk, M.L. Bruening, Highly selective separations of multivalent and monovalent cations in electrodialysis through nafion membranes coated with polyelectrolyte multilayers, Polymer 103 (2016) 478–485.

[20] N. White, M. Misovich, A. Yaroshchuk, M.L. Bruening, Coating of nafion membranes with polyelectrolyte multilayers to achieve high monovalent/divalent cation electrodialysis selectivities, ACS Appl. Mater. Interfaces 7 (2015) 6620–6628.

[21] M. Ahmad, S. Hussain, M.A. Abid, A. Mumtaz, M. Ibrar, S. Muhammad, Creating bipolar junction by depositing ultrathin anion-exchange coating on CationExchange membrane to dissociate water in electrodialysis, J. Membr. Sci. Res. 8 (2022) -.

[22] I. Stenina, D. Golubenko, V. Nikonenko, A. Yaroslavtsev, Selectivity of transport processes in ion-exchange membranes: relationship with the structure and methods for its improvement, Int. J. Mol. Sci. 21 (2020) 5517.

[23] R. Kingsbury, S. Zhu, S. Flotron, O. Coronell, Microstructure determines water and salt permeation in commercial ion-exchange membranes, ACS Appl. Mater. Interfaces 10 (2018) 39745–39756.

[24] C. Tang, M.L. Bruening, Ion separations with membranes, J. Polym. Sci. 58 (2020) 2831–2856.

[25] S. Aguilar, S. Bustillos, S. Xue, C.-H. Ji, W.H. Mak, E. Rao, B.T. McVerry, E.C. La Plante, D. Simonetti, G. Sant, Enhancing polyvalent cation rejection using perfluorophenylazide-grafted-copolymer membrane coatings, ACS Appl. Mater. Interfaces 12 (2020) 42030–42040.

[26] H. Zhang, Q. He, J. Luo, Y. Wan, S.B. Darling, Sharpening nanofiltration: strategies for enhanced membrane selectivity, ACS Appl. Mater. Interfaces 12 (2020) 39948–39966.

[27] Y. Huang, J. Sun, D. Wu, X. Feng, Layer-by-layer self-assembled chitosan/PAA nanofiltration membranes, Sep. Purif. Technol. 207 (2018) 142–150.

[28] S.J. Percival, S. Russo, C. Priest, R.C. Hill, J.A. Ohlhausen, L.J. Small, S.B. Rempe, E.D. Spoerke, Bio-inspired incorporation of phenylalanine enhances ionic selectivity in layer-by-layer deposited polyelectrolyte films, Soft Matter 17 (2021) 6315–6325.

[29] N.K. Mishra, N. Patil, S. Yi, D. Hopkinson, J.C. Grunlan, B.A. Wilhite, Highly selective hollow fiber membranes for carbon capture via in-situ layer-by-layer surface functionalization, J. Membr. Sci. 633 (2021), 119381.

[30] E. Guzman, R.G. Rubio, F. Ortega, A closer physico-chemical look to the layer-by-layer electrostatic self-assembly of polyelectrolyte multilayers, Adv. Colloid Interf. Sci. 282 (2020), 102197.

[31] M. Khavani, P. Batys, S.M. Lalwani, C.I. Eneh, A. Leino, J.L. Lutkenhaus, M. Sammalkorpi, Effect of ethanol and urea as solvent additives on PSS–PDADMA polyelectrolyte complexation, Macromolecules 55 (2022) 3140–3150.

[32] L. Ge, B. Wu, Q. Li, Y. Wang, D. Yu, L. Wu, J. Pan, J. Miao, T. Xu, Electrodialysis with nanofiltration membrane (EDNF) for high-efficiency cations fractionation, J. Membr. Sci. 498 (2016) 192–200.

[33] V. Gil, M. Porozhnyy, O. Rybalkina, K. Sabbatovskiy, V. Nikonenko, Modification of a heterogeneous cation-exchange membrane by ti-si based particles to enhance electroconvection and mitigate scaling during electrodialysis, Electrochim. Acta 391 (2021), 138913.

[34] W. Yu, D. Song, W. Chen, H. Yang, Antiscalants in RO membrane scaling control, Water Res. 183 (2020), 115985.

[35] J. Saqib, I.H. Aljundi, Membrane fouling and modification using surface treatment and layer-by-layer assembly of polyelectrolytes: state-of-the-art review, J. Water Process Eng. 11 (2016) 68–87.

[36] S. Abdu, M.-C.S. Martí-Calatayud, J.E. Wong, M. García-Gabaldón, M. Wessling, Layer-by-layer modification of cation exchange membranes controls ion selectivity and water splitting, ACS Appl. Mater. Interfaces 6 (2014) 1843–1854.

[37] J. Lambert, M. Avila-Rodriguez, G. Durand, M. Rakib, Separation of sodium ions from trivalent chromium by electrodialysis using monovalent cation selective membranes, J. Membr. Sci. 280 (2006) 219–225.

[38] J. Pan, J. Ding, R. Tan, G. Chen, Y. Zhao, C. Gao, B. Van der Bruggen, J. Shen, Preparation of a monovalent selective anion exchange membrane through constructing a covalently crosslinked interface by electro-deposition of polyethyleneimine, J. Membr. Sci. 539 (2017) 263–272.

[39] H. Zhang, R. Ding, Y. Zhang, B. Shi, J. Wang, J. Liu, Stably coating loose and electronegative thin layer on anion exchange membrane for efficient and selective monovalent anion transfer, Desalination 410 (2017) 55–65.

[40] H. Liu, H. Ruan, Y. Zhao, J. Pan, A. Sotto, C. Gao, B. Van der Bruggen, J. Shen, A facile avenue to modify polyelectrolyte multilayers on anion exchange membranes to enhance monovalent selectivity and durability simultaneously, J. Membr. Sci. 543 (2017) 310–318.

[41] Y. Zhao, K. Tang, H. Liu, B. Van der Bruggen, A.S. Díaz, J. Shen, C. Gao, An anion exchange membrane modified by alternate electro-deposition layers with enhanced monovalent selectivity, J. Membr. Sci. 520 (2016) 262–271.

[42] E. Belashova, N. Melnik, N. Pismenskaya, K. Shevtsova, A. Nebavsky, K. Lebedev, V. Nikonenko, Overlimiting mass transfer through cation-exchange membranes modified by nafion film and carbon nanotubes, Electrochim. Acta 59 (2012) 412–423.

[43] C. Cheng, N. White, H. Shi, M. Robson, M.L. Bruening, Cation separations in electrodialysis through membranes coated with polyelectrolyte multilayers, Polymer 55 (2014) 1397–1403.

[44] T. Ormanci-Acar, M. Mohammadifakhr, N.E. Benes, W.M. de Vos, Defect free hollow fiber reverse osmosis membranes by combining layer-by-layer and interfacial polymerization, J. Membr. Sci. 610 (2020), 118277.

[45] J.J. Richardson, J. Cui, M. Bjornmalm, J.A. Braunger, H. Ejima, F. Caruso, Innovation in layer-by-layer assembly, Chem. Rev. 116 (2016) 14828–14867.

[46] C. Cheng, A. Yaroshchuk, M.L. Bruening, Fundamentals of selective ion transport through multilayer polyelectrolyte membranes, Langmuir 29 (2013) 1885–1892.

[47] A.J. Bard, L.R. Faulkner, Fundamentals and applications, Electrochem. Methods 2 (2001) 580–632.

[48] E. Fontananova, W. Zhang, I. Nicotera, C. Simari, W. van Baak, G. Di Profio, E. Curcio, E. Drioli, Probing membrane and interface properties in concentrated electrolyte solutions, J. Membr. Sci. 459 (2014) 177–189.

[49] S. Mulyati, R. Takagi, A. Fujii, Y. Ohmukai, H. Matsuyama, Simultaneous improvement of the monovalent anion selectivity and antifouling properties of an anion exchange membrane in an electrodialysis process, using polyelectrolyte multilayer deposition, J. Membr. Sci. 431 (2013) 113–120.

[50] M. Vaselbehagh, H. Karkhanechi, R. Takagi, H. Matsuyama, Surface modification of an anion exchange membrane to improve the selectivity for monovalent anions in electrodialysis–experimental verification of theoretical predictions, J. Membr. Sci. 490 (2015) 301–310.

[51] X.-L. Wang, M. Wang, Y.-X. Jia, B.-B. Wang, Surface modification of anion exchange membrane by covalent grafting for imparting permselectivity between specific anions, Electrochim. Acta 174 (2015) 1113–1121.

[52] S. Abdu, K. Sricharoen, J.E. Wong, E.S. Muljadi, T. Melin, M. Wessling, Catalytic polyelectrolyte multilayers at the bipolar membrane interface, ACS Appl. Mater. Interfaces 5 (2013) 10445–10455.
[53] J.B. Schlenoff, H. Ly, M. Li, Charge and mass balance in polyelectrolyte multilayers, J. Am. Chem. Soc. 120 (1998) 7626–7634.
[54] J.J. Harris, J.L. Stair, M.L. Bruening, Layered polyelectrolyte films as selective, ultrathin barriers for anion transport, Chem. Mater. 12 (2000) 1941–1946.
[55] N. Parveen, M. Schönhoff, Swelling and stability of polyelectrolyte multilayers in ionic liquid solutions, Macromolecules 46 (2013) 7880–7888.
[56] L. Ouyang, R. Malaisamy, M.L. Bruening, Multilayer polyelectrolyte films as nanofiltration membranes for separating monovalent and divalent cations, J. Membr. Sci. 310 (2008) 76–84.
[57] G.M. Geise, D.R. Paul, B.D. Freeman, Fundamental water and salt transport properties of polymeric materials, Prog. Polym. Sci. 39 (2014) 1–42.